A&A 479, 149–154 (2008)
DOI: 10.1051/0004-6361:20078540

Astronomy & Astrophysics

Relation between CH cation and neutral/molecular hydrogen *(Research Note)*

T. Weselak[1], G. Galazutdinov[2], F. Musaev[3], and J. Krełowski[4]

[1] Department of Physics, Kazimierz Wielki University, Weyssenhoffa 11, 85-072 Bydgoszcz, Poland
e-mail: towes@ukw.edu.pl
[2] Korea Astronomy and Space Science Institute, Optical Astronomy Division, 61-1 Hwaam-Dong, Yuseong-Gu, Daejeon 305-348, Korea
e-mail: gala@kasi.re.kr
[3] Special astrophysical observatory, Nizhnij Arkhyz 369167, Russia
e-mail: faig@sao.ru
[4] Center for Astronomy, Nicolaus Copernicus University, Gagarina 11, Pl-87-100 Toruń, Poland
e-mail: jacek@astri.uni.torun.pl

Received 24 August 2007 / Accepted 28 November 2007

ABSTRACT

Observations of interstellar absorption bands of CH^+ molecule at 3957 and 4232 Å were applied to determine column densities toward 53 stars. The targets were selected because the atomic and molecular hydrogen column densities are published. The data on CH^+ were acquired using four echelle spectrographs situated in both the Northern and Southern hemispheres. Spatial relations between column densities of CH^+ and those of molecular, atomic and total hydrogen show large scatter, suggesting there is no relation between abundances of methylidyne cation and hydrogen in any form.

Key words. ISM: molecules – ISM: abundances

Introduction

The methylidyne cation (CH^+) was one of the first molecules discovered in the interstellar medium (ISM) by Douglas & Herzberg (1941) and since that time its formation and existence in ISM remains an unsolved problems. Many theoretical models have tried to reproduce its column densities, which are greater than 10^{12} cm^{-2} along a large number of lines of sight toward O and B stars (Black et al. 1975; Gredel et al. 1993).

The CH^+ molecule can be relatively easily observed from ground-based observatories because its 3957 and 4232 Å lines arising in the (0, 0) and (1, 0) bands of the $A^1\Pi - X^1\Sigma^+$ system. The first studies of this molecule demonstrated that it should vary linearly with atomic hydrogen (Federman 1982), however a problem with this relation, basing on observational results, remains. A relation between abundances of CH^+ and CH molecules shows a large scatter (Gredel 1997), however this result is based on relatively scarce observational material and needs to be further investigated.

High-resolution studies of CH^+ molecule (Crane et al. 1995; Crawford et al. 1995; Pan et al. 2004) have shown a complicated Doppler structure seen also in profiles of CH molecule which is closely related to molecular hydrogen (Weselak et al. 2004). These high-resolution data prove that components showing either CH but not CH^+, and CH^+ but not CH are exceptional. At lower spectral resolution essentially every CH component has a corresponding CH^+ component (Crawford 1995). The abundance of the CH molecule is closely related to that of KI (Welty & Hobbs 2001), and Doppler components seen in CH are also seen in KI, in most cases.

The mission of the Copernicus satellite showed that the H_2 molecule is relatively rich in diffuse and translucent clouds (Savage et al. 1977) with abundances exceeding 10^{19} cm^{-2} toward the examined OB stars. This result was also proven by another set of column densities, based on the data acquired with the FUSE satellite (Rachford et al. 2002; Pan et al. 2004; Burgh et al. 2007; Cecchi-Pestellini 2007).

Column densities of CH^+ molecule have different values in different literature datasets. In certain cases the compiled column densities of CH^+, given at the website http://astro.uchicago.edu/home/web/welty/coldens.html differ from those published in the paper of Crane et al. (1995). This was the case for HD 149757 which is a very popularly observed target. Such differences motivate new research, based on statistically meaningful samples of spectra – sets of homogeneous measurements, not on compilations only.

The recent study of the CH^+ molecule and hydrogen by Falgarone et al. (2005) suggested a close relation between column densities of CH^+ and total (atomic and molecular) hydrogen (their Fig. 2), based on measurements compiled results which were mostly taken from the literature and submillimeter observations of the CH^+ molecule. In this paper, we study the suggested relation between the abundance of CH^+ and that of the total, atomic and molecular hydrogen. The CH^+ abundances along 53 lines of sight were derived from our spectra of OB stars.

The observational data

Our observational material, listed in Table 1, was obtained during several observing runs between 1999 and 2007 using four echelle spectrographs:

The first is the MAESTRO fed by the 2-m telescope of the Observatory at Peak Terskol (TE) in the Northern Caucasus (Musaev et al. 1999); see also http://www.terskol.com/telescopes/3-camera.htm). The spectrometer is equipped with a Wright Instruments CCD 1242 × 1152 matrix (pixel size

Table 1. Observational and measurement data. Given are: star name (observed at t – Terskol (Russia), f – FEROS, H – HARPS La Silla (Chile), b – Bohyunsan (S.Korea)), spectral and luminosity class, reddening, *EW*s (mÅ) of CH^+ at 3597 Å and 4232 Å, column densities of CH^+ (obtained on the basis of f-values equal to 0.00331 and 0.00545 respectively), and column density of H_2 and H_{tot}. Data for hydrogen were taken from Savage et al. (1977), in case of: ^{R} – Rachford et al. (2002), ^{C} – Cecchi-Pestellini 2007, ^{P} – Pan et al. (2004), ^{B} – Burgh et al. (2007). With ^{x} – we designate lines of sight in case of which $N(CH^+)$ was obtained on the basis of unsaturated 3957 Å line.

HD	Sp/L	$E(B-V)$	EW(3957) [mÅ]	EW(4232) [mÅ]	$N(CH^+)$ [10^{12} cm^{-2}]	$N(H_2)$ [10^{20} cm^{-2}]	$N(H_{tot})$ [10^{20} cm^{-2}]
2905 ^{t}	B1Ia	0.34	—	11.3 ± 0.4	13.08 ± 0.46	1.88	19.80
10516 ^{t}	B2Vpe	0.17	—	3.0 ± 0.5	3.47 ± 0.57	0.12	3.72
21856 ^{b}	B1V	0.17	5.0 ± 0.4	8.6 ± 0.3	9.95 ± 0.34	1.10	13.20
22951 ^{t}	B0.5V	0.24	—	9.6 ± 0.3	11.11 ± 0.34	2.90	16.80
23180 ^{t}	B1III	0.27	4.3 ± 0.4	5.8 ± 0.2	6.71 ± 0.23	4.00	16.10
24398 ^{t}	B1Iab	0.29	—	3.9 ± 0.5	4.51 ± 0.57	4.70	15.80
24534 ^{t}	O9.5pe	0.56	2.5 ± 0.3	4.3 ± 0.4	4.98 ± 0.46	8.32^R	13.68
24760 ^{t}	B0.5V	0.07	—	2.3 ± 0.3	2.66 ± 0.34	0.34	3.16
24912 ^{t}	O7.5Iab	0.30	—	20.8 ± 0.4	24.07 ± 0.46	3.40	19.80
27778 ^{b}	B3V	0.37	4.9 ± 0.3	9.3 ± 0.4	10.76 ± 0.46	6.17^R	15.71
30614 ^{t}	O9.5Ia	0.25	—	14.9 ± 0.4	17.25 ± 0.46	2.19	12.40
36861 ^{b}	O8III	0.10	—	0.56 ± 0.1	0.65 ± 0.11	0.13	6.31
40111 ^{b}	B1Ib	0.13	2.1 ± 0.3	3.5 ± 0.2	4.05 ± 0.23	0.55	9.12
46150 ^{f}	06e	0.45	7.2 ± 0.3	13.1 ± 0.4	15.16 ± 0.46	3.85^C	22.70
47129 ^{f}	O8e	0.33	10.5 ± 0.4	18.3 ± 0.4	21.18 ± 0.46	3.50	19.00
48099 ^{f}	O6	0.25	12.5 ± 0.3	17.7 ± 0.4	20.49 ± 0.46	1.95	17.90
53975 ^{f}	O8V	0.18	—	2.4 ± 0.3	2.78 ± 0.34	0.17	14.30
54662 ^{f}	O6	0.33	6.1 ± 0.3	10.3 ± 0.4	11.92 ± 0.46	1.00	26.00
61347 ^{f}	O9.5Iab	0.45	9.8 ± 0.4	17.5 ± 0.5	20.25 ± 0.57	4.20^C	42.47
110432 ^{f}	B2pe	0.48	8.2 ± 0.2	13.9 ± 0.4	16.09 ± 0.46	4.37	11.44
112244 ^{f}	O9Ib	0.24	3.7 ± 0.2	6.8 ± 0.3	7.87 ± 0.34	1.38	14.80
113904 ^{f}	WR	0.18	2.8 ± 0.2	5.9 ± 0.3	6.83 ± 0.34	0.68	13.40
135591 ^{f}	O7Iab	0.18	3.8 ± 0.3	6.6 ± 0.3	7.64 ± 0.34	0.59	13.20
143275 ^{f}	B0.2IV	0.12	—	2.7 ± 0.2	3.12 ± 0.23	0.26	14.50
144217 ^{H}	B0.5V	0.16	2.98 ± 0.05	5.11 ± 0.07	5.91 ± 0.08	0.67	13.70
144470 ^{f}	B1V	0.18	4.1 ± 0.2	6.2 ± 0.2	7.18 ± 0.23	1.12	17.30
145502 ^{f}	B2IV	0.26	3.4 ± 0.2	6.0 ± 0.2	6.94 ± 0.23	0.78	15.60
147165 ^{H}	B1III	0.34	3.07 ± 0.03	5.28 ± 0.06	6.11 ± 0.07	0.62	23.20
147933 ^{H}	B2V	0.45	7.5 ± 0.2	13.1 ± 0.2	15.16 ± 0.23	3.70	72.00
148184 ^{H}	B2Vne	0.48	7.24 ± 0.04	9.98 ± 0.03	11.55 ± 0.03	4.30	22.60
148605 ^{f}	B3V	0.11	—	1.3 ± 0.1	1.50 ± 0.11	0.05	9.10
149038 ^{f}	B0Ia	0.24	16.1 ± 0.4	26.7 ± 0.4	35.09 ± 0.87^x	2.75	15.60
149757 ^{H}	O9.5V	0.28	14.2 ± 0.3	23.5 ± 0.4	31.19 ± 0.15^x	4.40	14.10
150898 ^{f}	B0Iab	0.14	6.3 ± 0.3	10.8 ± 0.3	12.50 ± 0.34	0.65	10.30
151804 ^{f}	O9e	0.35	5.6 ± 0.3	9.6 ± 0.4	11.11 ± 0.46	1.82	15.60
152234 ^{f}	B0.5Ia	0.42	12.6 ± 0.3	22.2 ± 0.6	27.46 ± 0.65^x	2.70^C	23.01
152408 ^{f}	O7pe	0.45	7.1 ± 0.2	11.0 ± 0.3	12.73 ± 0.34	2.40	22.80
154368 ^{f}	O9.5Iab	0.73	11.0 ± 0.3	17.5 ± 0.4	20.25 ± 0.46	14.45	24.45
155806 ^{f}	O9	0.28	5.0 ± 0.3	8.0 ± 0.2	9.26 ± 0.23	0.83	13.80
164353 ^{t}	B5Ib	0.10	5.2 ± 0.7	11.33 ± 1.5	11.33 ± 1.52	1.83	13.80
184915 ^{t}	B0.5III	0.19	—	6 ± 0.2	6.94 ± 0.23	2.05	12.02
203064 ^{t}	O8V	0.25	—	4.1 ± 0.2	4.75 ± 0.23	1.98	14.00
203374 ^{t}	B0IVpe	0.60	—	5.7 ± 0.7	6.60 ± 0.08	5.01^P	—
203938 ^{t}	B0.5IV	0.70	14.6 ± 0.5	26.2 ± 0.6	31.82 ± 1.09^x	10.00^R	40.20
206267 ^{t}	O6	0.49	8.0 ± 0.4	10.0 ± 0.3	11.57 ± 0.34	7.24^R	27.20
207198 ^{t}	O9II	0.55	—	17.6 ± 0.3	20.37 ± 0.34	6.76^R	28.63
207538 ^{b}	B0V	0.59	—	4.8 ± 0.3	5.56 ± 0.34	8.13^R	30.00
209975 ^{t}	O9.5Ib	0.31	12.5 ± 0.5	23.5 ± 0.5	27.24 ± 1.09^x	1.20	15.40
210839 ^{t}	O6e	0.56	6.0 ± 0.4	9.3 ± 0.3	10.76 ± 0.34	6.92^R	21.03
217035 ^{t}	B0V	0.76	20.6 ± 0.7	37.3 ± 1.0	44.90 ± 1.53^x	9.00^P	—
218376 ^{b}	B0.5IV	0.21	3.4 ± 0.5	8.3 ± 0.7	9.61 ± 0.80	1.41	11.80
224572 ^{b}	B1V	0.17	4.2 ± 0.4	8.2 ± 0.5	9.49 ± 0.57	1.70	10.90
303308 ^{f}	B1III	0.30	6.6 ± 0.4	10.2 ± 0.7	11.81 ± 0.23	2.24^B	—

22.5 μm × 22.5 μm) camera. The instrument forms échelle spectra which cover the range from 3500 to 10 100 Å, divided into up to 92 orders. The existing set of gratings and cameras allows several resolutions: from R = 45 000 through 80 000 to 120 000. In this project we used the R = 80 000 resolution as a kind of compromise: it allows us to see discrepancies of the profiles from single Gaussians and also – to observe relatively heavily reddened stars.

The second one, covering the Southern hemisphere, is the Feros spectrograph, fed with the 2.2-m ESO telescope (see- `http://www.ls.eso.org/lasilla/sciops/2p2/E2p2M/FEROS`). The resolution of these spectra, covering the Southern hemisphere, is constant (R = 48 000). This instrument allows us to record the whole available spectral range (~3700–9200 Å, divided into 37 orders) in a single exposure. The flatfielding can be very precise in the case of Feros as it is the fiber-fed spectrograph; this is not important while measuring *EW*s of reasonably narrow features but may be important in cases of reasonably broad DIBs.

The most recent observations were carried out using the fiber-fed echelle spectrograph installed at the 1.8-m telescope of the Bohyunsan Optical Astronomy Observatory (BOAO) in South Korea. The spectrograph has three observational modes providing resolving power 30 000; 45 000 and 90 000. In all cases, it allows recording of the whole spectral range from ~3500 to ~10 000 Å divided into 75–76 spectral orders. We used the highest resolution mode in our project.

The spectra of five objects were obtained with the HARPS spectrometer, fed wi6th the 3.6-m ESO telescope in Chile (see `http://www.ls.eso.org/lasilla/sciops/3p6/harps/`). This spectrograph allows us to cover the range ~3800–~6900 Å with the resolution R = 115 000. As the instrument designed to search for exoplanets, it guarantees very precise wavelength measurements.

All spectra were reduced using the standard packages: MIDAS and IRAF as well as our own DECH code (Galazutdinov 1992) which provides all standard procedures of image and spectra processing. The use of different computer codes for the data reduction procedures reduces the possibility of inaccuracies following slightly different ways of dark subtraction, flatfielding or excision of cosmic ray hits.

For this project we used the sample of 53 stars for which column densities of atomic and molecular hydrogen are published in the literature. In Table 1 we present the HD number, spectral type and luminosity class as well as the $E(B-V)$ color excess for each star, *EW*s (mÅ) of CH^+ 3957 and 4232 lines, calculated column densities on the basis of unsaturated line and column densities of molecular and total hydrogen which were taken from the literature. In the case of the line with $EW < 20$ mÅ, the saturation effects can be neglected (van Dishoeck & Black 1989). Column densities of 3957 and 4232 lines were obtained on the basis of f-values equal to 0.0031 and 0.00545 respectively (Larsson & Siegbahn 1983). $E(B-V)$s were estimated on the basis of average colour indices currently available in the SIMBAD database and the intrinsic color indices published by Papaj et al. (1993).

Results

In Fig. 1 we present the CH^+ line at 4232 Å in spectra of four stars of similar reddening. The evident scatter of the intensity of the molecular ion feature confirms its weak relation to $E(B-V)$ – already demonstrated by Krełowski et al. (1999). Additional components in the profiles of 4232 line are seen in the cases

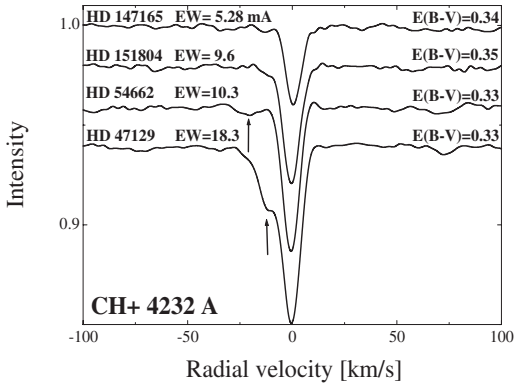

Fig. 1. Profiles of CH^+ line at 4232 Å in spectra of four stars of similar reddening. Strengths of 4232 line increase from top to bottom. The additional component in the profile of HD 54662 and 47129 is clearly visible.

of HD 54662 and 47129. It is not possible to check whether dust particles, causing reddening, populate all clouds, revealed by CH^+ Doppler components, or only some of them since one can estimate only the total extinction along any line of sight.

Our measurements of *EW*s of CH^+ features at 3957 and 4232 Å were made in spectra characterized by different resolutions. In Fig. 2 we compare profiles of CH^+ at 4232 Å, CH at 4300 Å and KI atomic line at 7699 Å in spectra of three stars in the radial velocity scale. The comparison demonstrates that CH^+ features are not simply correlated with the other two lines. The CH^+ components are often stronger while those of CH and KI are relatively weak. This suggests that CH^+ is likely to occupy different than CH or KI regions of ISM.

Observed abundances of CH^+ molecule can be explained by shock models with temperatures higher than 1000 K genearted by shock waves with speeds of order of the 10 km s^{-1} (Gredel et al. 1993). The shock models also predict velocity shifts between CH and CH^+, which are not observed (see Snow & McCall 2006). However, in Fig. 3 we present the spectrum of HD 207198 where the velocity shift between CH and CH^+ is observed (in the case of HD 204827 and 210839 velocity shifts were also detected in our spectra).

Our measurements were compared with those published in the compilation of Krełowski et al. (1999, Fig. 4); in cases of multiple results the average value was calculated for each star. Our results are closely related to those published previously, as seen in Fig. 4.

We would like to emphasize that in the case of strong features (EW > 20 mÅ) the saturation effects may be essential (van Dishoeck & Black 1989). Fortunately, the weaker 3957 Å line of CH^+ can be measured in this case to obtain column density without any risk of saturation. In this way we obtain column density of CH^+ based on 3957 Å line if 4232 Å is saturated. To obtain column density we used the relation of van Dishoeck & Black (1989) in the case of lines which were unsaturated: $N = 1.13 \times 10^{20}\ EW/(\lambda^2 f)$, where EW and λ are in Å and column density in cm^{-2}.

We would like to emphasize that in the case of relatively weak CH^+ lines, one can use *EW*s instead of column density without a risk of saturation effect. In Fig. 5 we present the correlation between stronger CH^+ 4232 and weaker 3957 Å line. This relation is linear and the strength ratio of these two lines is close to 1.6. The range of linearity appears much broader than expected (i.e. *EW*s are simply proportional to column densities

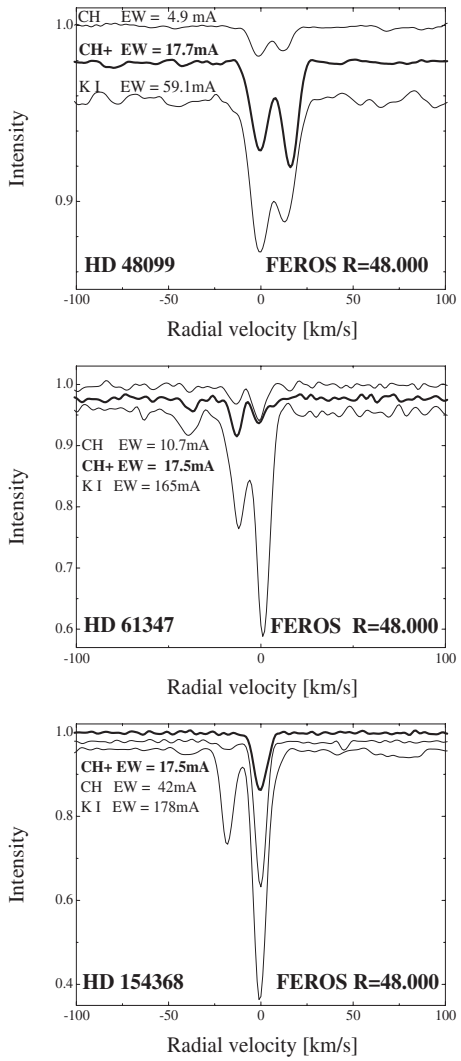

Fig. 2. A comparison of CH (4300 Å), CH^+ (4232 Å) and KI (7699 Å) profiles in spectra of HD 48099, 61347 and 154368. The CH^+ profile is plotted with a bold line in each figure. Intensity ratios in profile components differ in the case of CH^+ and KI (HD 48099, 61347).

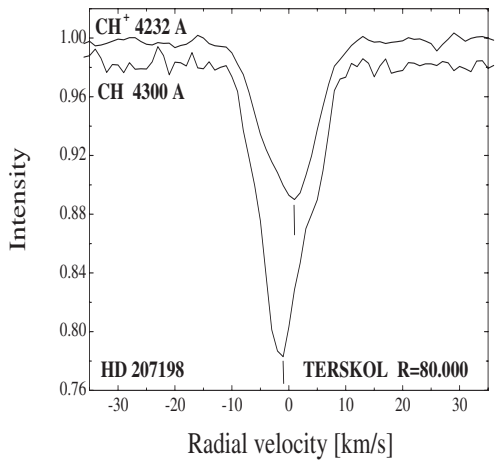

Fig. 3. A comparison of profiles of CH and CH^+ molecules at 4300 and 4232 Å in the spectrum of HD 207198. The velocity shift is clearly visible.

even while they exceed the limit of 20 mÅ). This is likely because of the effect seen in Fig. 1; the Doppler splitting prevents

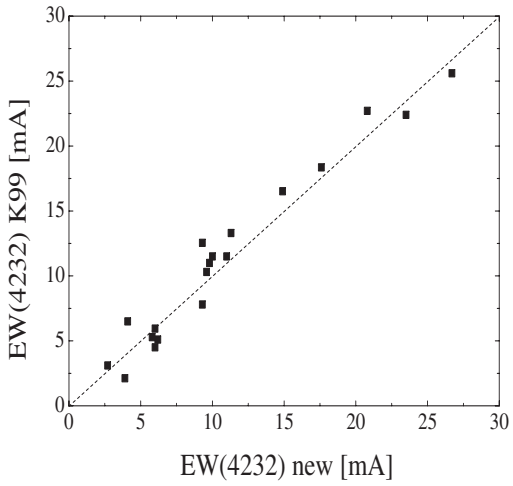

Fig. 4. A comparison of our equivalent width measurements of CH^+ 4232 line with those taken from compilation of Krełowski et al. (1999). The relation is very good and equal to 45°.

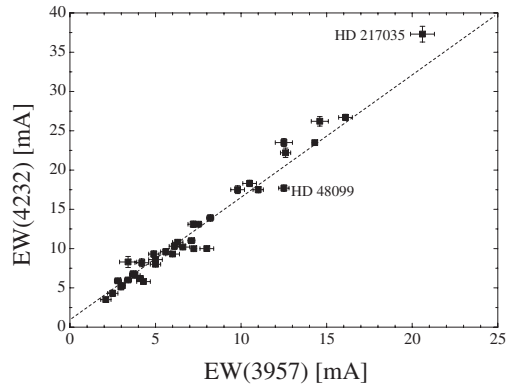

Fig. 5. Correlation plot between equivalent widths of the CH^+ 4232 and 3957 line; as measured in our spectra. Linear relation proves the lack of any saturation effects.

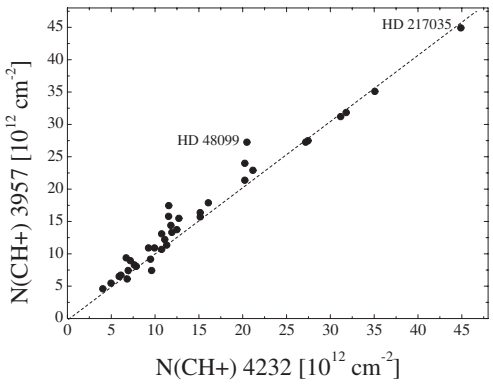

Fig. 6. Correlation plot between column densities obtained on the basis of the CH^+ 3957 and 4232 lines. The small systematic difference is seen, but the relation is very good.

the saturation effects appearing from even in relatively strong lines.

In Fig. 6 we relate column densities of the CH^+ molecule obtained on the basis of the 3957 and 4232 lines. The small saturation effects can probably be seen only in the case of HD 217035

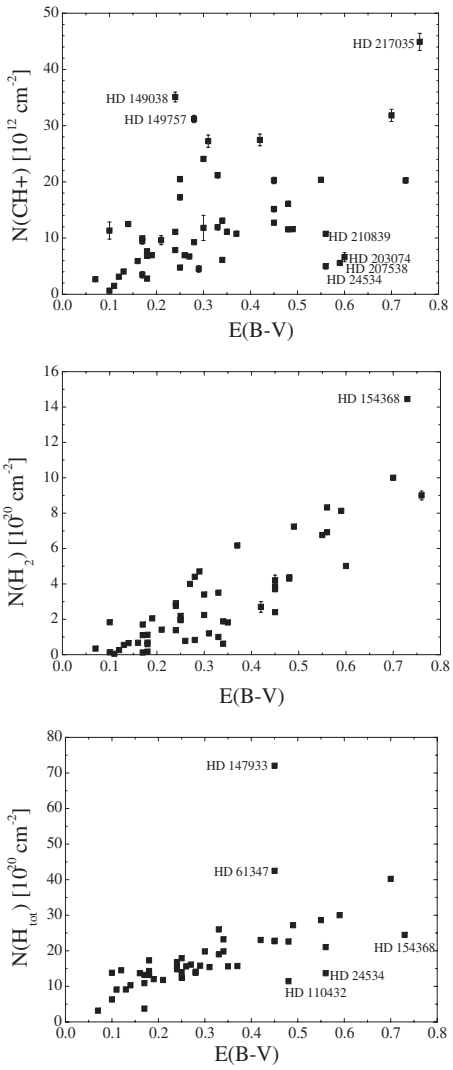

Fig. 7. Correlation plots between column densities of CH^+ (at the *top*) H_2 (in the *middle*) and H_{tot} (*bottom*) and $E(B-V)$. The better relation with $E(B-V)$ is more clearly seen in the case of molecular hydrogen and total hydrogen than the CH^+ molecule.

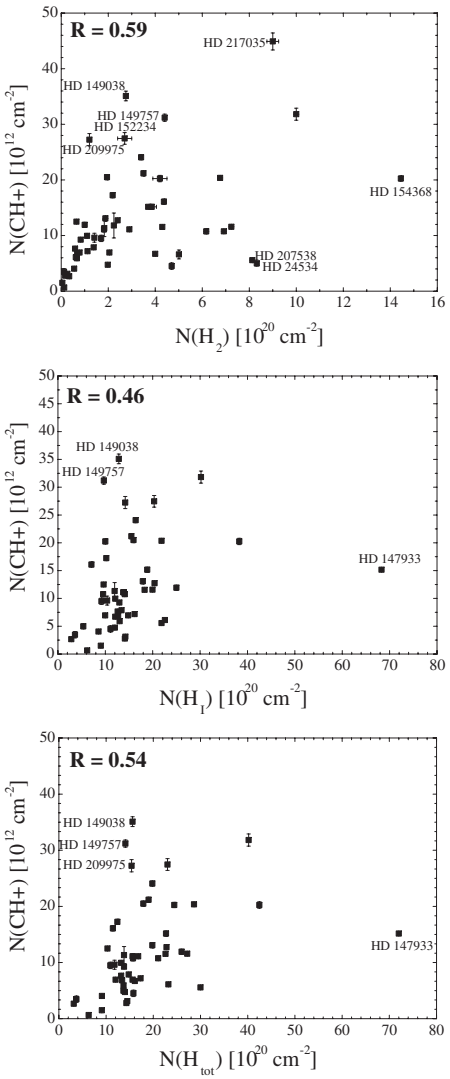

Fig. 8. Correlation patterns between column densities of CH^+ molecule and H_2 (at the *top*), HI (in the *middle*) and H_{tot} – *bottom*. Very poor relation with correlation coefficient equal to 0.59, 0.46, 0.54 is seen in each plot respectively.

with the highest value of column density. At this point we have to stress that in many cases the observed interstellar features are composed of many Doppler components which, even if not resolved, make the lines unsaturated up to relatively high equivalent widths.

The collected data on 53 lines of sight allow us to relate column densities of CH^+ to $E(B-V)$ in Fig. 7. The two quantities apparently correlate very poorly. Even if an average relation exists, many data-points are highly discrepant. Contrary to this, column density of CH molecule and reddening are well correlated (Weselak et al. 2004). In Fig. 7 we also demonstrate the relations between abundances of molecular and total hydrogen, and $E(B-V)$. They are much tighter with only one missing point in the case of relation between column density of the total hydrogen and reddening (HD 147933 is the star obscured by ρ Oph cloud, with very high value of H I).

In Fig. 8 we present correlation plots between column density of CH^+ and, as published previously, column densities of hydrogen in molecular, atomic and total form. In each case the relations are very poor with correlation coefficients equal to 0.59, 0.46 and 0.54, respectively. Apparently methylidyne cation is not spatially related to neutral and/or molecular hydrogen. Both species occupy different clouds of different physical conditions. This is the main conclusion of this paper. We emphasize that, according to Megier et al. (2005), carriers of different interstellar absorption features may occupy different regions of the interstellar medium. A proper interpretation of any interstellar absorption spectrum requires that features originating in the same environment be related. Relations between column densities of spectral features carried by simple molecular species such as CH, CN, C_2 or CO are not tight which suggests different chemistry from cloud to cloud. It seems important to analyze such relations, based on new samples of homogeneous measurements from optical, UV and infrared spectra of OB stars. It is certainly important to collect more spectra of high signal-to-noise ratio to obtain correct values of column densities and check to what extent simple molecules are related to each other. The other requirement is that of high resolution as only such spectra allow resolution of Doppler components which are blended in most of our spectra.

Acknowledgements. The authors acknowledge the following financial support: JK acknowledges that of the Polish State during the period 2007−2010 (grant N203 012 32/1550).

References

Black, J. H., Dalgarno, A., & Oppenheimer, M. 1975, ApJ, 199, 633
Burgh, E. B., France, K., & McCandliss, S. R. 2007, ApJ, 658, 446
Cecchi-Pestellini, C. 2007, Private Communication
Crawford, I. A. 1995, MNRAS, 277, 458
Crane, P., Lambert, D. L., & Sheffer, Y. 1995, ApJS, 99, 107
Douglas, A. E., & Herzberg, G. 1941, ApJ, 94, 381
Falgarone, E., Phillips, T. G., & Pearson, J. C. 2005, ApJ, 634, L149
Federman, S. R. 1982, ApJ, 257, 125
Galazutdinov, G. A. 1992, Prep. Spets. Astrof. Obs., No 92
Gredel, R. 1997, A&A, 320, 929
Gredel, R., van Dishoeck, E. F., & Black, J. H. 1993, A&A, 269, 477
Krełowski, J., Ehrenfreund, P., Foing, B. H., et al. 1999, A&A, 347, 235
Larsson, M., & Siegbahn, P. E. M. 1983, Chem. Phys., 76, 175
Megier, A., Strobel, A., Bondar, A., et al. 2005, ApJ, 634, 451
Musaev, F. A., Galazutdinov, G. A., Sergeev, A. V., Karpov, N. V., & Podyachev, Yu. V. 1999, Kinematika Fiz. Nebesn. Tel, 15, No. 3
Pan, K., Federman, S. R., Cunha, K., Smith, V. V., & Welty, D. E. 2004, ApJS, 151, 313
Papaj, J., Krełowski, J., & Wegner, W. 1993, A&A, 273, 575
Rachford, B. L., Snow, T. P., Tumlinson, J., et al. 2002, ApJ, 577, 221
Savage, B. D., Bohlin, R. C., Drake, J. F., & Budich, W. 1977, ApJ, 216, 291
Snow, T. P., & McCall, B. J. 2006, ARA&A, 44, 367
van Dishoeck, E. F., & Black, J. H. 1989, ApJ, 340, 273
Welty, D. E., & Hobbs, L. M. 2001, ApJS, 133, 345
Weselak, T., Galazutdinov, G. A., Musaev, F. A., & Krełowski, J. 2004, A&A, 414, 949